

A PRELIMINARY STUDY OF CERTAIN ELECTRICAL PROPERTIES  
OF STANNIC OXIDE CERAMICS

By

HERMAN EXCELL MATTHEWS, JR.

Bachelor of Science

Lamar State College of Technology

1962

Submitted to the faculty of the Graduate School of  
the Oklahoma State University  
in partial fulfillment of the requirements  
for the degree of  
MASTER OF SCIENCE  
May, 1965

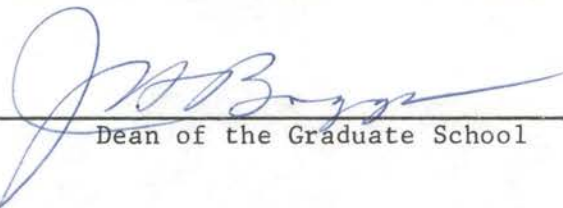
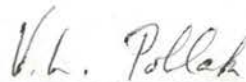
SEP 21 1966

A PRELIMINARY STUDY OF CERTAIN ELECTRICAL PROPERTIES  
OF STANNIC OXIDE CERAMICS

Thesis Approved:



Thesis advisor



Dean of the Graduate School

587615

## ACKNOWLEDGMENT

The author wishes to express his deepest gratitude to Dr. E. E. Kohnke for his patience and guidance throughout the execution of this work and to the National Aeronautics and Space Administration for support in the form of a student traineeship. He is also indebted for use of equipment to J. Houston who designed the equipment and to J. Houston and H. Kunkle for helpful suggestions during the course of the investigation.

## TABLE OF CONTENTS

Chapter	Page
I. INTRODUCTION . . . . .	1
II. PREPARATION AND DESCRIPTION OF SAMPLES . . . . .	3
Forming Process . . . . .	3
Firing Process . . . . .	4
Cleaning and Tapping Techniques . . . . .	8
III. CAPACITANCE MEASUREMENTS . . . . .	10
Measurement Equipment and Procedure . . . . .	10
Results . . . . .	12
IV. CONDUCTANCE MEASUREMENTS . . . . .	18
Dark Conductance . . . . .	18
Photoconductance . . . . .	21
V. CONCLUSIONS AND SUGGESTIONS FOR FURTHER STUDY . . . . .	30
Firing and Forming Process . . . . .	30
Microstructure of Ceramics . . . . .	31
Conductance Properties (Dark) . . . . .	31
Conductance Properties (Light) . . . . .	32
BIBLIOGRAPHY . . . . .	34

## LIST OF TABLES

Table	Page
I. Sample Dimensions and Composition . . . . .	12

## LIST OF FIGURES

Figure		Page
1. Relative density as a function of firing time at a fixed firing temperature . . . . .		6
2. Relative density as a function of firing temperature at a fixed firing time . . . . .		7
3. Equivalent representative circuits for a dielectric sample		14
4. Dielectric constant as a function of measuring frequency .		15
5. Resistivity as a function of measuring frequency . . . . .		16
6. Dark conductivity as a function of reciprocal temperature for a pure sample . . . . .		19
7. Dark conductivity as a function of reciprocal temperature for a doped sample . . . . .		20
8. Current as a function of impressed voltage . . . . .		22
9. Photodecay transient . . . . .		23
10. Thermally stimulated current as a function of temperature for a doped sample . . . . .		25
11. Thermally stimulated current as a function of temperature for a pure sample . . . . .		27
12. Continuous thermal quenching . . . . .		29

## CHAPTER I

### INTRODUCTION

In recent years there have been many studies of the electrical and optical properties of metal oxides in crystalline, thin film, and pressed powder forms. Extensive work has been done at Oklahoma State University on both natural and artificial stannic oxide crystals (1) and this investigation is presently being extended to include stannic oxide in ceramic form. The adaptability of ceramics to sizing and shaping and their high surface area make them particularly suitable for the investigation of surface phenomena and possibilities for correlation with bulk electrical measurements in stannic oxide are most promising since high quality synthetic crystals of this material can be produced locally (2).

The purpose of the following report is to give the results obtained in a preliminary study of these ceramics which was undertaken to develop sample preparation techniques and to evaluate a number of experimental methods as to their pertinence and utility in characterizing basic parameters. A recent account of certain stannic oxide ceramic bulk properties has been given by Loch (3) and an interesting example of related work is provided by Lewis (4) who has been studying the behavior of cadmium telluride in ceramic form and comparing it with bulk crystal results.

As might be expected, the first major problem encountered in producing suitable ceramic specimens was to develop forming techniques and

determine optimum firing conditions for both "pure" (composed of reagent-grade powder) and "doped" (containing added impurities) stannic oxide bodies. Although these measurements were essentially exploratory in nature, they did bring to light some interesting and important basic problems involving ceramics. They will be described in Chapters II and V.

The first set of electrical measurements made on these samples determined their capacitance and resistance as a function of frequency. It was hoped that these measurements might prove useful for probing differences between the physical characteristics of ceramics and single crystals. An analytical analysis is suggested by A. Von Hippel (5) and will be discussed farther in Chapter III.

The most significant and potentially important measurements made on these samples were the conductance measurements. In addition to determinations of the "dark" conductance temperature dependence in a range from  $-150^{\circ}\text{C}$  to  $200^{\circ}\text{C}$ , several procedures which are part of a group of experimental techniques identified in the literature as a "photoelectronic analysis"\* were applied to selected specimens. Quantities measured were spectral response, photoconductance decay transients, thermally stimulated currents, and thermal quenching. A description of these experiments and the conclusions drawn from them will be discussed in Chapters IV and V.

---

\*See, for example, Bube, R. H., Photoconductivity of Solids, John Wiley and Sons, New York (1960).

## CHAPTER II

### PREPARATION AND DESCRIPTION OF SAMPLES

Since literature concerning the preparation of stannic oxide ceramics is extremely sketchy, much of the actual preparation of suitable samples was simply a trial and error procedure. The problem divided itself into two main parts: forming the stannic oxide pellets and determining correct firing or maturing conditions.

#### Forming Process

The equipment used for the forming of the pellets consisted of a hydraulic Carver Laboratory Press capable of exerting forces from 1,000 to 24,000 lbs and a powder compression chamber made by the departmental shop. Using this particular press and die arrangement, the powder could be subjected to pressures of 5,000 to 120,000 psi. In the compression, it was found that the powder stuck to the faces of the die causing irregularities in both the surfaces and the bulk of the pellets. To reduce this, the faces of the die were ground and polished as flat and smooth as possible using number 600 grit paper and crocus cloth, and they were thoroughly cleaned before each compression of powder.

All ranges of pressures from hand tamping to 100,000 psi were tried to eliminate internal faults in the resultant samples. The lower pressures left the samples too fragile, and the higher pressures produced



large cracks in the interior. After many trials it was found that pressures from 10,000 to 15,000 psi produced the best samples, although there still remained the problem of small defects along the outer edges of the pellets. Such defects were probably caused by a slight bit of play in the powder press; but suitable samples were readily obtained by sorting the pressed pellets.

The final method of preparing samples for heat treatment may be outlined as follows:

- (a) Mix stannic oxide powder in an acetone slurry, stirring continuously until gummy.
- (b) Dry this mixture in air at room temperature for 24 hours.
- (c) Press the residue in small pellets using pressures from 10,000 to 15,000 psi.

This procedure gave pellets that were extremely cohesive and had densities of about 4 gm/cc ready for firing.

Since this investigation was not limited to pure stannic oxide ceramics but was extended to doped samples, a description of doping techniques is needed. The stannic oxide powder and the powder to be used in the doping were carefully weighed and then the dry powders were mixed thoroughly. Because this didn't assure uniformity, the composite powder was mixed with acetone forming a slurry and put in a sealed container. This container was placed on a reciprocating "shaker" for about two days and then the above procedure starting at (b) was followed.

#### Firing Process

The next major problem was the correct firing or maturing process. When fabricating samples to be used for optical and electrical

measurements, it is desirable to obtain as high density samples as possible to minimize problems of handling, shaping, etc. The theoretical density of rutile-structure  $\text{SnO}_2$ , using lattice constants  $a = 4.72 \text{ \AA}$  and  $c = 3.16 \text{ \AA}$  (6) and the atomic mass of two  $\text{SnO}_2$  molecules, is  $7.11 \text{ gm/cc}$ . A typical single crystal grown in the lab was found to have a density of  $7.02 \pm 0.12 \text{ gm/cc}$ , which is in excellent agreement with the calculated theoretical density, while a natural cassiterite crystal from Bolivia might have a density as low as  $6.62 \text{ gm/cc}$ . One would like to have densities of the fired ceramics as close to these numbers as possible.

When firing a ceramic there are four main variables that can determine the maturity of the sample: (1) amount and kind of impurity in the powder, (2) procedure of heat treatment before and after the maximum firing temperature is reached, (3) maximum firing temperature, and (4) time at maximum firing temperature. Figure 1 shows the relationship of relative density (the ratio of the measured density to the theoretical density) to firing time for a fixed firing temperature of  $1246^\circ \text{ C}$ . Figure 2 shows the relationship of relative density to firing temperature for a fixed firing time of 4 hours. From Figures 1 and 2, optimum firing conditions in terms of least time and temperature for the zinc-doped samples can be set at  $1350^\circ \text{ C}$  for 25 hours. However, there seems to be no significant dependence of density on firing time or temperature for the pure reagent-grade samples in the ranges studied. An extension of the time range has been made by Peterson (7) who fired a sample for 1,000 hours, but he achieved no significant increase in density over samples fired to the same temperature for less time. An extension of the temperature range by Goodman and Gregg (8) shows significant densification of

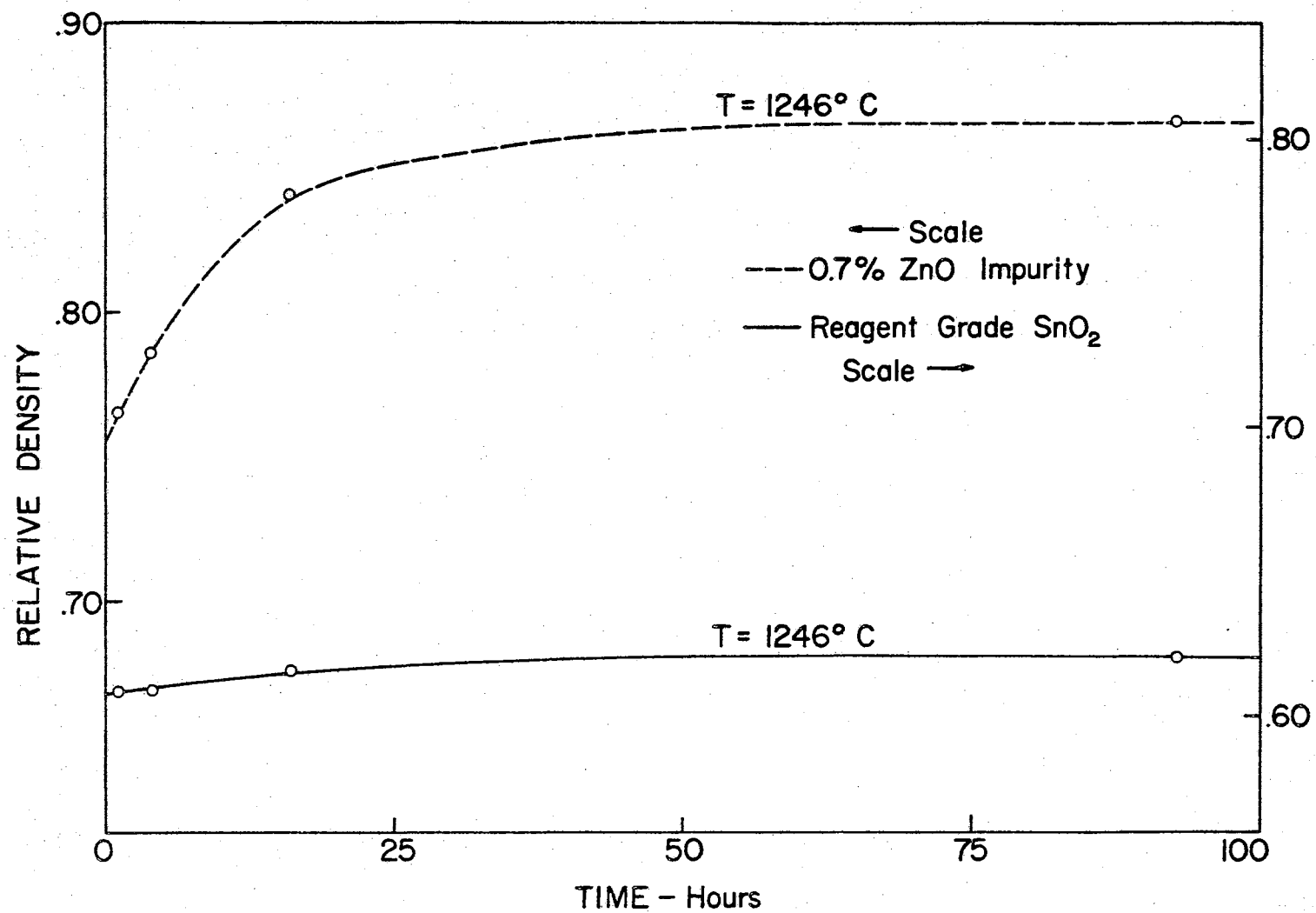


Figure 1. Relative density as a function of firing time at a fixed firing temperature

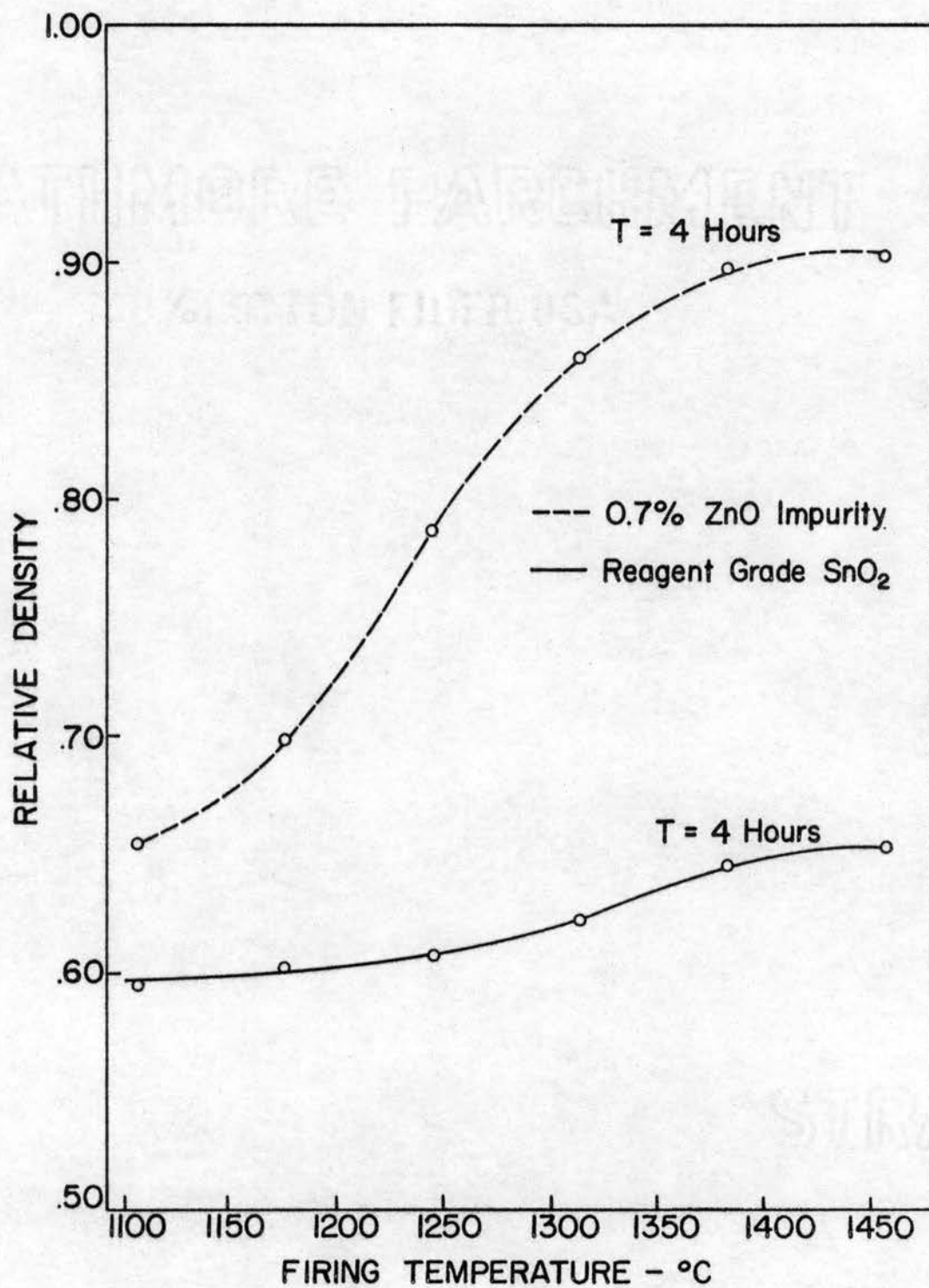


Figure 2. Relative density as a function of firing temperature at a fixed firing time

pure  $\text{SnO}_2$  powder at  $1600^\circ \text{C}$ . Confirmation of this result will be sought in the near future when installation of a gas fired furnace is completed. This equipment should materially extend the temperature range now available with an ordinary globar muffle furnace. Scattered measurements made on properties of comparable low density pure  $\text{SnO}_2$  ceramics have also been reported by Lindner and Enquist (9) and Nomura (10).

#### Cleaning and Lapping Techniques

After the samples had been prepared and fired, they had to be thoroughly cleaned before making measurements. This necessarily entailed grinding the surfaces to remove any impurity introduced from the surroundings in which they were fired. Following much trial and error experience with different procedures, a method was established for both selecting good samples and cleaning them thoroughly. After samples were removed from the furnace they were visually inspected for any gross flaws and those that had none were placed in a Hoffman lapping machine, two at a time. These were lapped using a mixture of M303 Centriforce Abrasive and a silicone oil as the grinding compound. This size abrasive is commonly used for fine finishing; therefore, the mixture ground away the surfaces slowly leaving them flat and parallel in one operation. The samples were first lapped for a short period of time and then roughly cleaned in carbon tetrachloride using an ultrasonic cleaner. Subsequently, they were inspected under a binocular microscope for surface flaws. If none were visible the specimen was set aside; otherwise it was put back in the lapping machine. By continuing this process the samples were sorted until a few superior ones could be

chosen. These were thoroughly cleaned in carbon tetrachloride which removed nearly all the visible part of the abrasive mixture. Finally, they were heated to  $850^{\circ}$  C for 12 hours to completely dry them and to remove the rest of the residue abrasive mixture from the surface.

#### Color and Size of Samples

The selected samples then had extremely clean, uniform surfaces suggesting a uniform bulk density. The color of the individual sample appeared to be dependent on the firing temperature. It was found that pure samples heated above a temperature somewhere between  $1380^{\circ}$  C to  $1460^{\circ}$  C turned a pink color which was uniform throughout the bulk while samples fired below this temperature were white or had only a slight pink hue. In the doped samples the pink color appeared at a much lower temperature, but proved to be only a surface phenomenon for all firing temperatures since the pink surface could be ground off leaving a white sample.

The physical dimensions of the samples were measured with a micrometer and the drum dial of the dielectric sample holder as explained later. They were then weighed using a Mettler balance and the density of each sample was calculated. Typical examples are tabulated in Chapter III.

## CHAPTER III

### CAPACITANCE MEASUREMENTS

#### Measurement Equipment and Procedures

All measurements were made on a Type 1610-A General Radio Capacitance Measuring Assembly of which the following components were used: a Type 716-C Capacitance Bridge, which is a Schering Bridge capable of measuring capacitances at frequencies from 30 cycles to 300 KC, a Type 1302-A Oscillator which has a frequency range from 10 cycles to 100 KC, a Type 1231-B Amplifier and Null Detector which uses a Type 1231-B Power Supply, and a Type 1231-P5 Filter which provides 30 to 45 db discrimination against noise. Since this assembly and all instructions for use are commercially accessible, no more will be said about circuitry except that an oscilloscope was used in place of the Null Detector. The most important additional instrument needed for measurement of small capacitances was the Dielectric Sample Holder.

A Type 1690-A Dielectric Sample Holder was used for all of the capacitance measurements on the bridge and as a device to measure the physical thickness of the samples. For the capacitance measurements the Sample Holder was placed, using a Type 1690-PL Adaptor, at the unknown substitutional terminals of the 716-C Capacitance Bridge and a variable air capacitor was used at the unknown direct terminals as a standard. The measurements of the sample thickness were made using the calibrated drum which adjusts the electrode spacing. Since



equations not derived in the instruction manual were used, a brief outline of these derivations and the procedure of operation will be given.

The electrode spacing is adjusted to the thickness of the sample  $t$  and the bridge is balanced with the empty Sample Holder at the unknown substitutional terminals. (Note: the variable air capacitor must be set at least 100 pf larger than the sample to be measured.) This reading  $C_1$  corresponds to the capacitance of the leads and sample holder  $C_o$  plus the air capacitance  $C_{at}$ . Next, the sample is centered in the Sample Holder and the bridge rebalanced. The new reading  $C_2$  corresponds to the capacitance of the leads and sample holder  $C_o$  plus the capacitance of the air  $C_a$  plus the capacitance of the sample  $C_x$ . The difference  $C_2 - C_1$  equals  $\Delta C = C_a + C_x - C_{at}$  or  $C_x = \Delta C + C_{at} - C_a$ . But  $C_a = C_{at}(1 - A_x/A)$  where  $A_x$  is area of the sample and  $A$  is area of the Sample Holder electrodes. Therefore

$$C_x = \Delta C + C_{at}(A_x/A). \quad (1)$$

If the samples are treated as parallel plate capacitors, their capacitance  $C_x$  can be written in terms of their geometry as  $C_x = K\epsilon_o A_x/t$  where  $K$  is the dielectric constant,  $\epsilon_o$  is the permittivity of free space,  $A_x$  is the area, and  $t$  is the thickness. Multiplying by  $A/A$  gives  $C_x = (K\epsilon_o A/t)(A_x/A)$  or  $C_x = KC_{at}(A_x/A)$ . Putting this back in equation (1) leads to  $KC_{at}(A_x/A) = \Delta C + C_{at}(A_x/A)$  or, finally,

$$K = \Delta C/C_{at}(A_x/A) + 1. \quad (2)$$

The value of  $C_{at}$  is directly calculable for any Sample Holder electrode spacing. This is the equation used for calculating dielectric constants from the measurements.



The bridge also measures the loss tangent of the particular sample, allowing its resistance or resistivity to be calculated. The loss tangent, or dissipation factor  $D$ , for a parallel RC circuit is equal to  $1/\omega C_x R_x$  where  $\omega$  is the angular measuring frequency,  $C_x$  is the unknown capacitance as calculated by equation (1), and  $R_x$  is the unknown resistance. Rearranging the expression and putting  $R_x$  and  $C_x$  in terms of  $\rho$ ,  $K$ , and geometrical quantities, gives

$$\rho = 1/\omega K \epsilon_o D. \quad (3)$$

This is the equation used for calculating the resistivity of the samples from the measurements.

The following table lists the physical dimensions and composition of two representative specimens used in capacitance measurements.

TABLE I  
SAMPLE DIMENSIONS AND COMPOSITION

Sample No.	Composition (by weight)	Thickness (mm)	Area (cm <sup>2</sup> )	Density (gm/cc)
2	Fisher Reagent Grade SnO <sub>2</sub>	2.17	1.18	4.55
8	0.7% ZnO 99.3% SnO <sub>2</sub>	1.53	0.957	6.48

### Results

When making standard AC bridge measurements of dielectric samples it is customary to characterize the specimen in terms of an equivalent circuit as shown in Figure 3a where  $C$  represents the capacitance and  $R$

the leakage. Measuring this capacitance and resistance as a function of the frequency of the applied field and eliminating geometrical factors as shown in the previous section leads to values for the dielectric constant and resistivity which are shown plotted as a function of frequency in Figures 4 and 5 for two representative ceramic specimens. When measurements were made on a single crystal grown in the lab, however, there was no dispersion of the dielectric constant and a reduced dispersion in the resistivity suggesting that at least part of the usual dispersion observed in ceramics may be due to their granular structure as opposed to the regular crystalline structure of the single crystal.

Looking at a ceramic sample as a large number of randomly oriented microcrystals fused together, Koops (11) suggested characterizing the sample by the use of the equivalent circuit shown in Figure 3b where  $R_1$ ,  $R_2$ ,  $C_1$ , and  $C_2$  are constants. The merit of this circuit lies in the fact that one might be able to qualitatively lump all the grain boundary properties into the top parallel RC circuit and all of the bulk properties of the grains into the lower circuit thereby giving these four constants some physical meaning.

Setting the circuit shown in Figure 3b equivalent to the circuit shown in Figure 3a, one obtains expressions for the measured  $R$  and  $C$  in terms of the four constants and the frequency as shown below:

$$C = \frac{1}{R_1 + R_2} \left[ \frac{\tau_1 + \tau_2 - \tau + \omega^2 \tau_1 \tau_2 \tau}{1 + \omega^2 \tau^2} \right] \quad (4)$$

$$R = \frac{(R_1 + R_2)(1 + \omega^2 \tau^2)}{1 + \omega^2 \tau_1 \tau_2 + \omega^2 \tau_1 \tau + \omega^2 \tau_2 \tau} \quad (5)$$

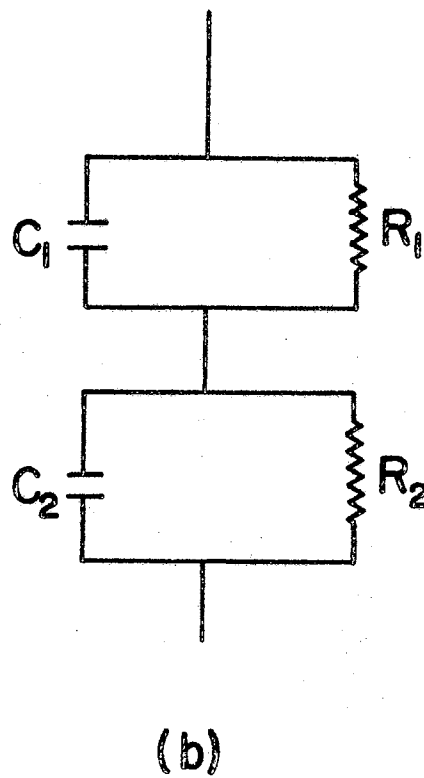
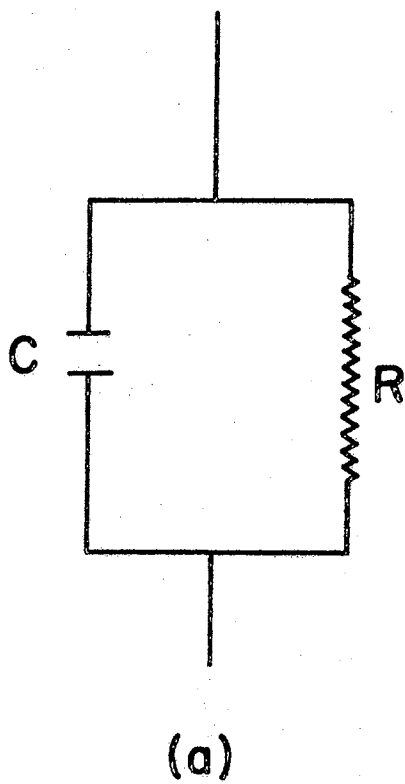


Figure 3. Equivalent representative circuits for a dielectric sample

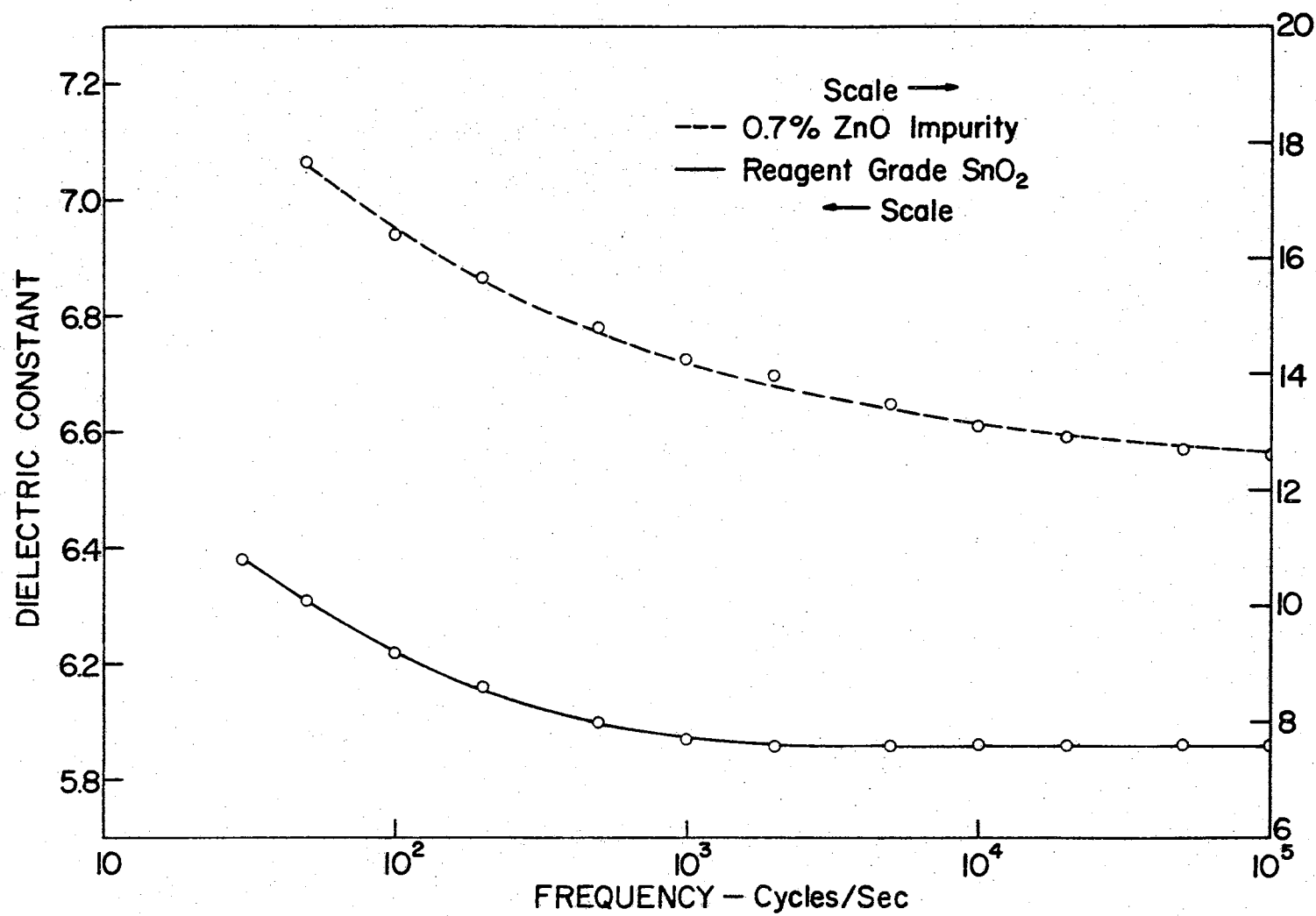


Figure 4. Dielectric constant as a function of measuring frequency

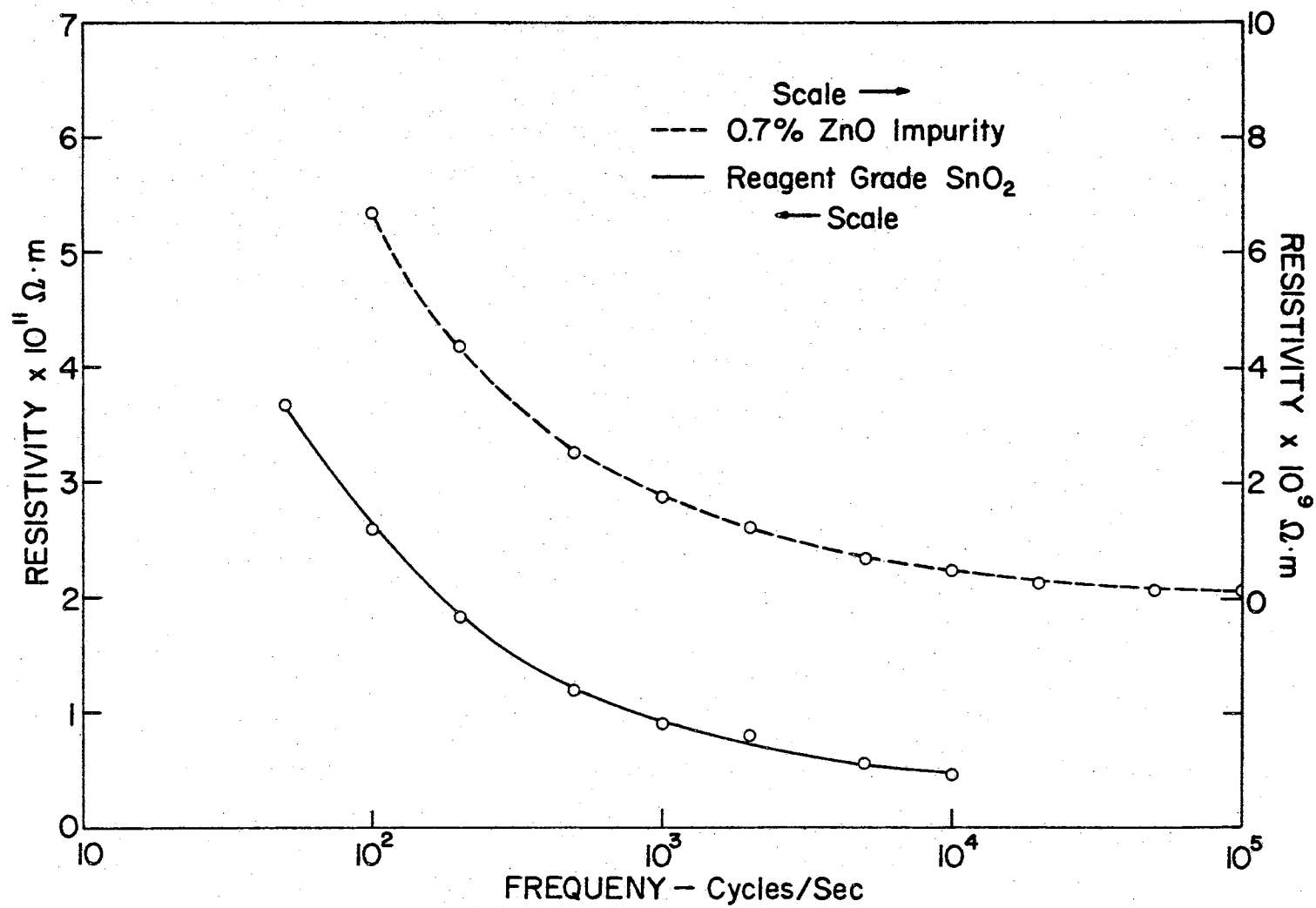


Figure 5. Resistivity as a function of measuring frequency

where  $\tau = R_1 R_2 (C_1 + C_2) / (R_1 + R_2)$ ,  $\tau_1 = R_1 C_1$ ,  $\tau_2 = R_2 C_2$ , and  $\omega$  is the angular measuring frequency. If this four-constant circuit is to be equivalent to that of Figure 3a, then algebraic manipulation of equations (4) and (5) shows that the ratio  $\{R(\omega_1)C(\omega_1) - R(\omega_2)C(\omega_2)\} / \{R(\omega_1) - R(\omega_2)\}$  must be a constant for all frequency values. Here  $R(\omega_1)$  and  $C(\omega_1)$  denote the experimental value of  $R$  and  $C$  evaluated at frequency  $(\omega_1)$  from Figures 4 and 5, etc. From the experimental data it was found for these particular ceramic samples that the above ratio deviated at most by 15% over the measured frequency range indicating that circuit 3b provides a reasonable, although not exact, equivalence to the experimental results.

It is evident that more complicated equivalent circuits could provide an improved fit since the number of adjustable parameters would be increased. At the present stage of the study, however, it is felt that no useful purpose would be served by increasing the equivalent circuit complexity since this would tend only to make the physical interpretation of the individual parameters increasingly obscure.

## CHAPTER IV

### CONDUCTANCE MEASUREMENTS

When performing conductance measurements on insulators, one must be careful in designing circuits and sample holders in order to minimize system leakage and the background noise level. The particular set of measurements described in this section was made using an electrometer circuit and a sample holder designed by Houston (12). The reference cited presents a thorough discussion of these problems and gives the details of appropriate experimental techniques.

#### Dark Conductance

The first measurements made on the ceramic samples were to determine the dark conductance dependence on temperature and the results are expressed in terms of sample current  $C_D$  for an impressed voltage of 90 volts. Figure 6 shows a plot of  $\log i_D$  versus  $10^3/T$  for a pure sample of density 4.4 gm/cc that was "fixed" thermally by heating it at 100° C in air for 4 to 5 hours. A calculation of an "activation energy"  $E_a$ , as defined by the equation  $i_D = \text{const } e^{-(E_a/2kT)}$ , gave a value of 1.58 ev. It should be noted in passing that equivalent measurements made on a pink sample originally fired to a higher temperature gave an  $E_a$  of 1.1 ev. Figure 7 shows a plot of  $\log i_D$  versus  $10^3/T$  measured in a rough pump vacuum for a doped sample (0.7% ZnO impurity by weight) of density of 6.2 gm/cc. The associated  $E_a$  was 0.92 ev. Before proceeding

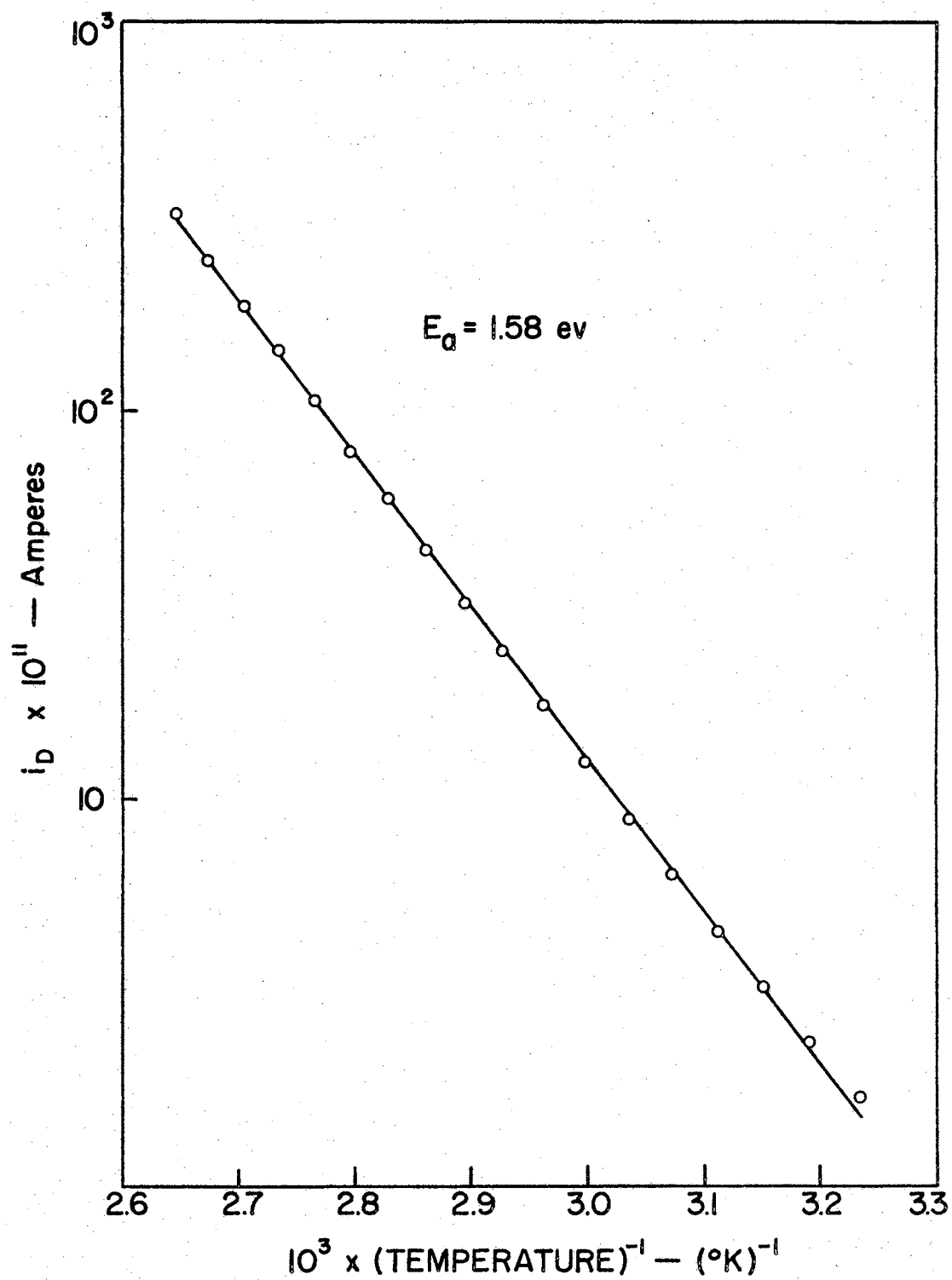


Figure 6. Dark conductivity as a function of reciprocal temperature for a pure sample.



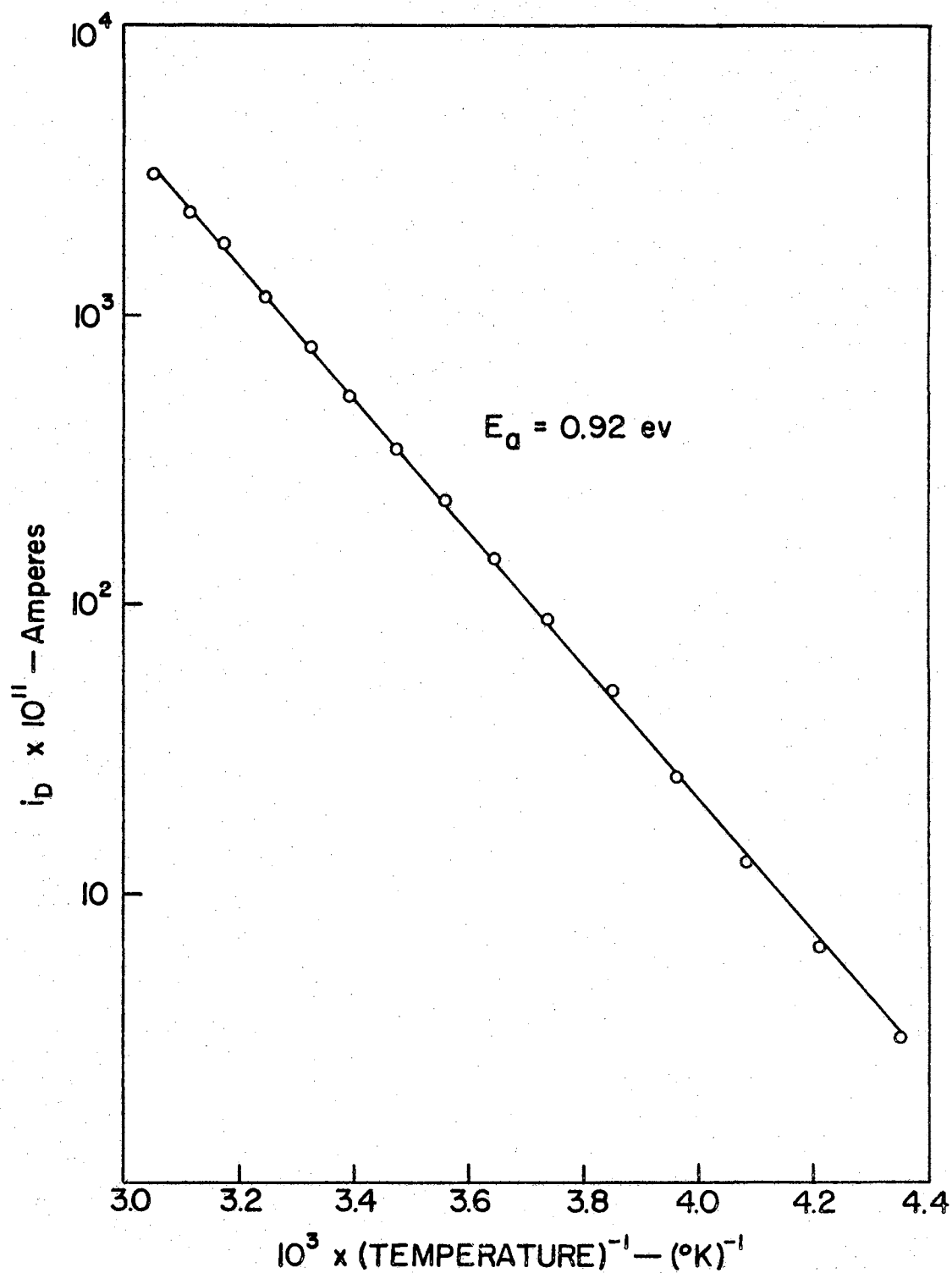


Figure 7. Dark conductivity as a function of reciprocal temperature for a doped sample.

to a discussion of the results of photoconductance measurements, it should be stated that silver paint\* contacts were used and were assumed to be ohmic in both the dark conductance and photoconductance measurements. As shown in Figure 8, this assumption appears to be valid.

### Photoconductance

When one is investigating impurity levels in a semiconductor or insulator by photoconductance techniques, a useful framework for the study of different impurity parameters is provided by a photoelectronic analysis. A complete analysis was not performed in this preliminary study, but the following paragraphs described the results of a partial analysis.

#### Spectral Response

Spectral response gives the dependence of photocurrent on exciting wavelength. Only the visible and near ultraviolet regions were inspected and a photoresponse peak was observed at approximately 300 mμ. Using this to estimate an intrinsic band gap leads to a value of approximately 4.0 ev, in excellent agreement with that obtained from grown sample measurements (12).

#### Photodecay

A typical plot of photodecay as a function of time for a pure  $\text{SnO}_2$  ceramic is shown in Figure 9. This was done both at atmospheric pressure and in a rough pump vacuum, and the differences are quite similar to those observed for photodecays of natural crystals under

---

\*The silver paint was electronic grade 4817 distributed by DuPont.

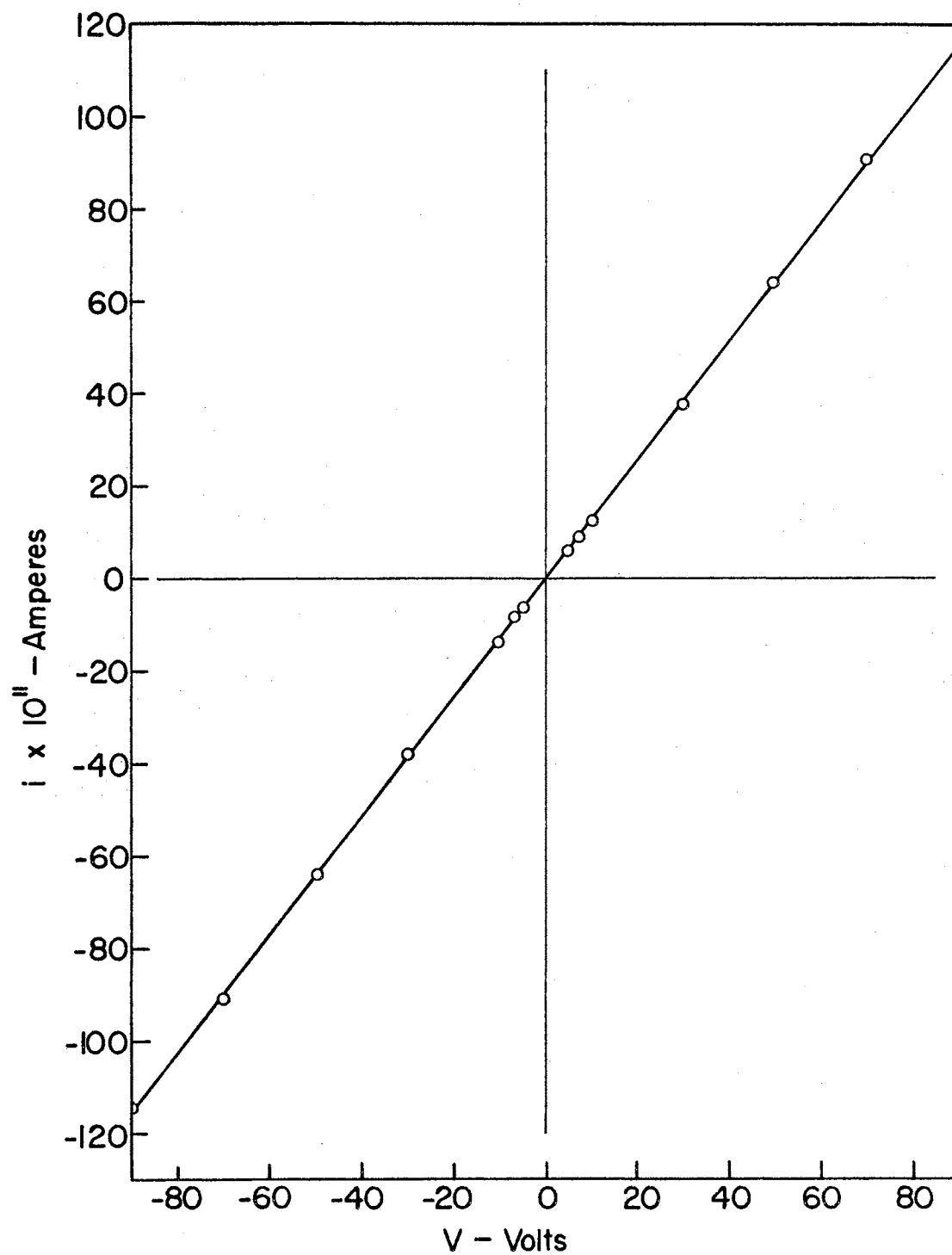


Figure 8. Current as a function of impressed voltage

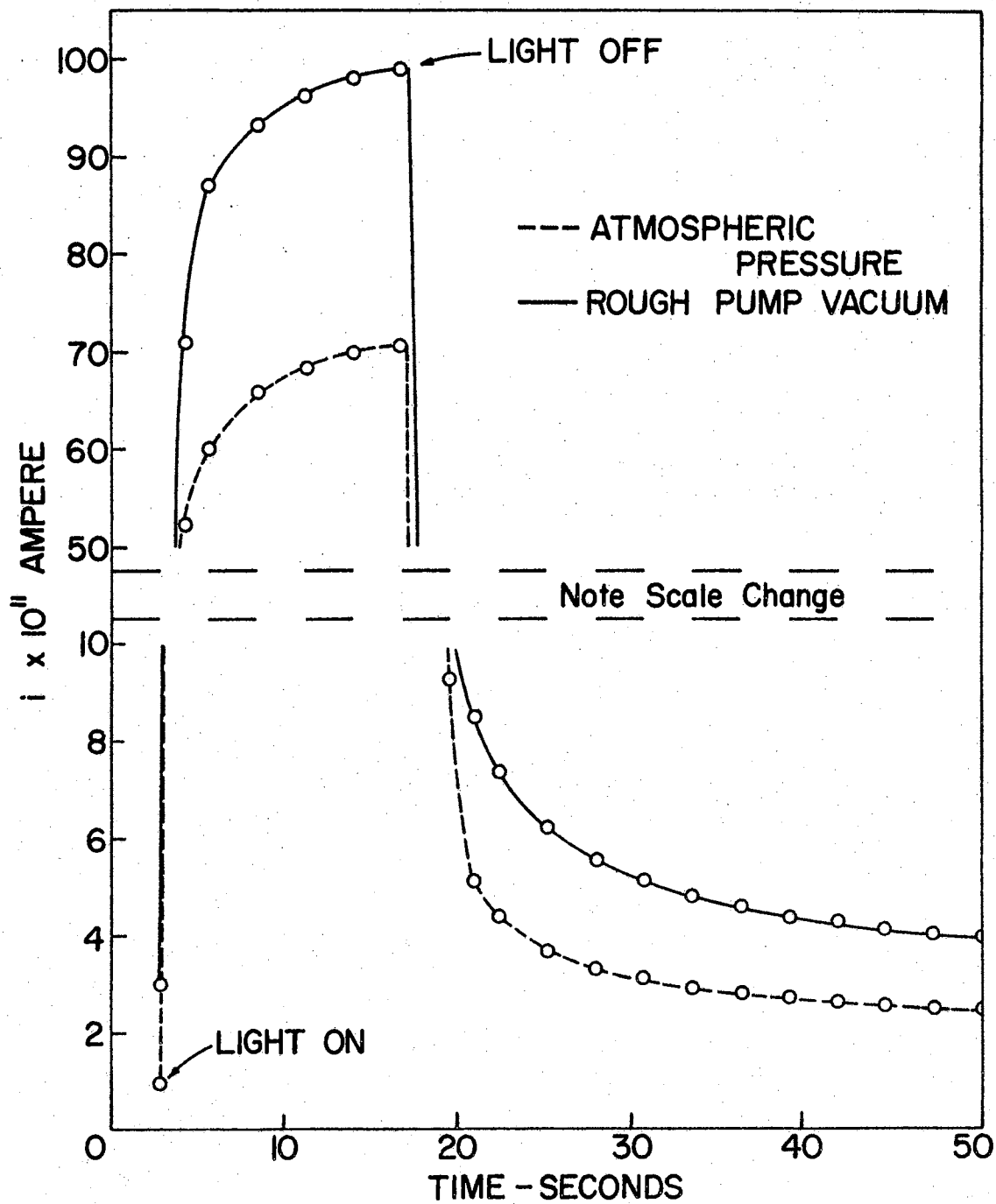


Figure 9. Photodecay transient

similar conditions (13), i.e., a lower current and faster decay in air than in the rough pump vacuum. Measurements of this type were also made on ZnO-doped ceramics and the qualitative results were the same.

#### Thermally Stimulated Currents

The technique of thermally stimulated current measurements is best described by the following outline of procedure:

- (a) Take the sample to a low temperature in the dark (in this case,  $-180^{\circ}\text{C}$ ).
- (b) Excite the sample with intrinsic radiation until saturated and allow to decay in the dark.
- (c) Slowly heat the specimen and record the current in the sample circuit as a function of the temperature (note the temperature rise of the sample should be linear in order to perform calculations from this data).
- (d) Plot the data as  $i_{\text{TSC}}$  versus temperature where  $i_{\text{TSC}}$  is the current recorded minus the dark current.

Figure 10 shows the graphic results for a ZnO-doped sample using this type of procedure. The phenomenological reason for the observed peak is as follows: the effect of (a) and (b) above is to trap a non-equilibrium density of carriers in one or more discrete energy levels at the low temperature and as the temperature rises, these levels empty, allowing the carriers to enter the conduction process. This means that each TSC peak should be in some way indicative of an individual trapping level emptied. A widely used method for determining this trapping activation energy is Bube's (14) steady-state Fermi level calculation which assumes that at the TSC peak the steady-state Fermi level coincides in energy with the trapping state. If one makes these assumptions,

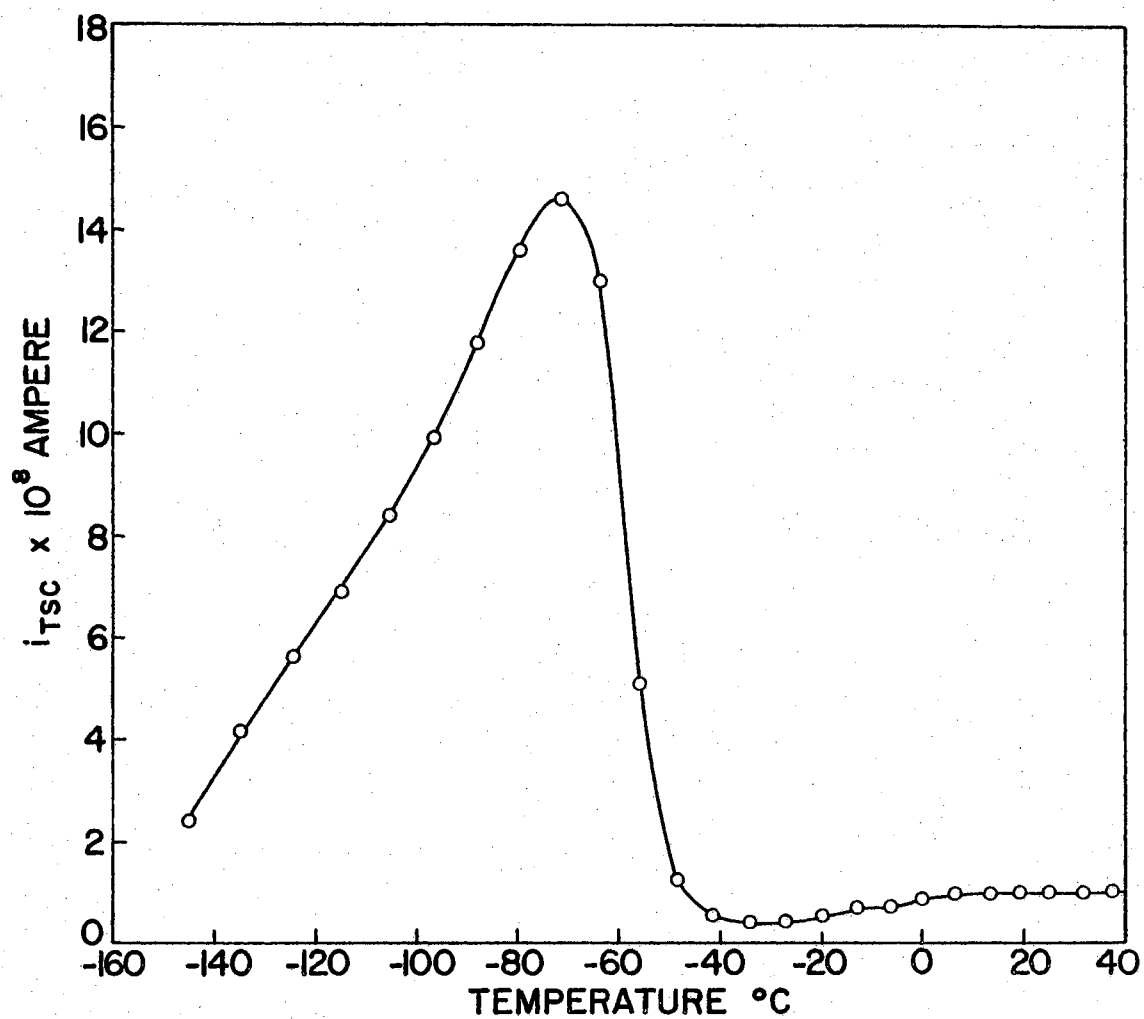


Figure 10. Thermally stimulated current as a function of temperature for a doped sample

the expression for the activation energy becomes

$$E_t = kT_m \ln \mu N_c e / \sigma(T_m) \quad (6)$$

where  $T_m$  and  $\sigma(T_m)$  are respectively the temperature and conductivity at the TSC peak,  $e$  is the electronic charge,  $k$  is Boltzmann's constant,  $\mu$  is the mobility, and  $N_c$  is the density of states in the conduction band. Assuming a value of  $N_c = 10^{19}/\text{cc}$  and  $\mu = 10 \text{ cm}^2/\text{volt-sec}$ , a calculation using the data in Figure 10 gives an activation energy of 0.38 ev. Although this method of calculating is open to question, it is not the purpose of the present work to evaluate the magnitudes obtained but rather to seek comparisons between samples.

When these same measurements were made on a pure sample, this low temperature peak was found to be a function of oxygen pressure as shown in Figure 11. Although the two peaks shown in this Figure are three orders of magnitude apart in conductivity and 40 degrees apart in temperature, a calculation using equation 6 gives a value of 0.50 ev for the high peak and 0.54 ev for the low peak. Another calculation of  $E_t$  taken from data on another pure sample gives a value of 0.48 ev. These results summarized then seem to say that for pure  $\text{SnO}_2$  there exists a TSC peak which has an average activation energy value of 0.51 ev and which varies in shape and position with oxygen pressure. Although the implications of this measurement are not fully appreciated as yet, it is felt it will provide a starting point for considering the effect of surface treatment and ambient gas pressure on trapping and/or recombination processes.

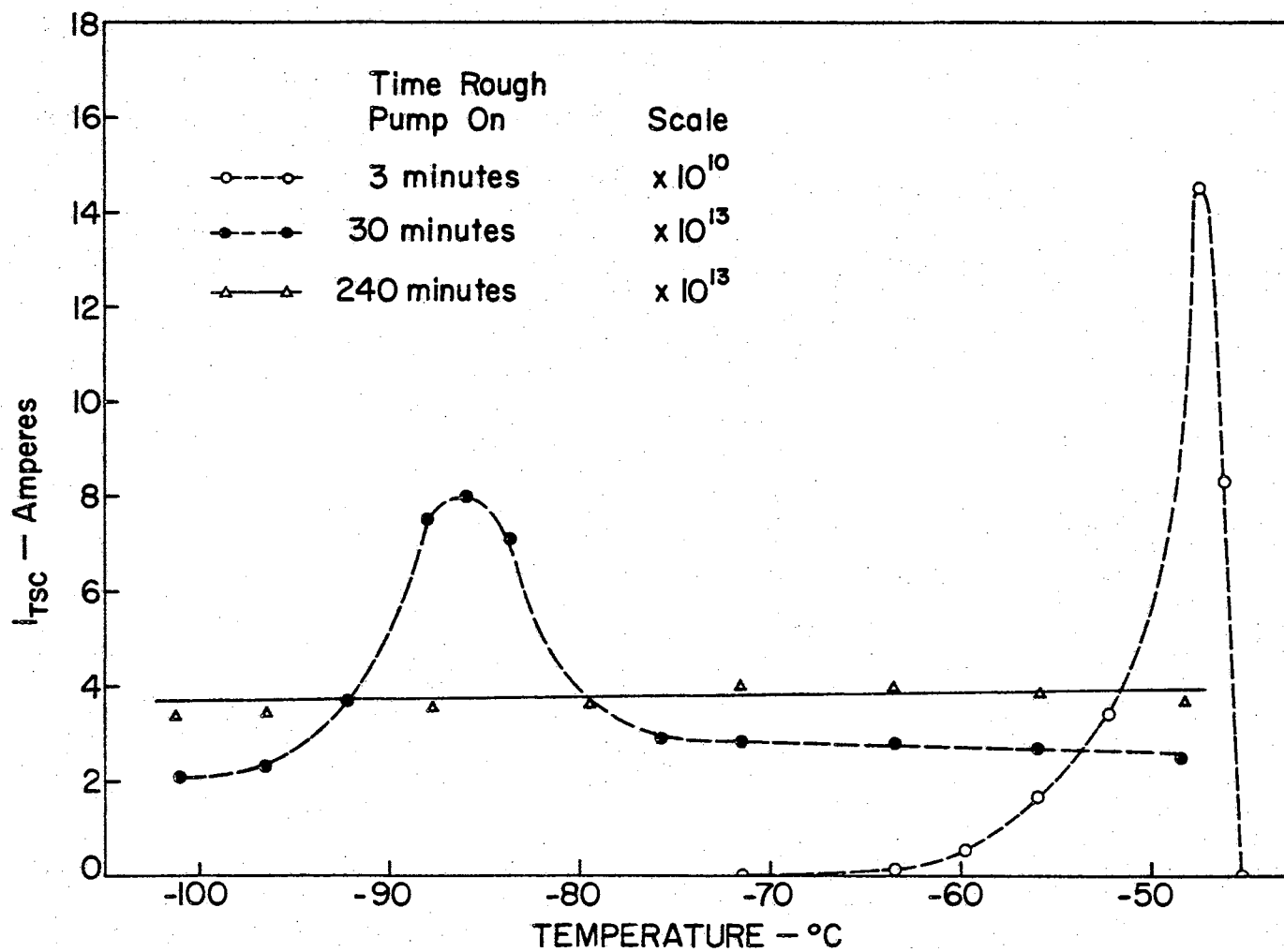


Figure 10. Thermally stimulated current as a function of temperature for a doped sample



### Thermal Quenching

The term thermal quenching describes a process in which an energy level switches from a trap to a recombination center at a particular temperature. The phenomenological picture was proposed by Rose and since no calculations were made from this data it will suffice to simply point out that a quantitative description of the phenomenon is found in Bube (14). Figure 12 gives the experimental results of two measurements of peak photocurrent versus temperature and shows that thermal quenching definitely exists for the doped samples but is not observable in pure samples over the temperature range investigated. It is inviting to speculate that the presence of zinc in the dope specimens introduces compensated acceptor levels which sensitize the photoconduction process at low temperatures. Further study using other dopants is anticipated.

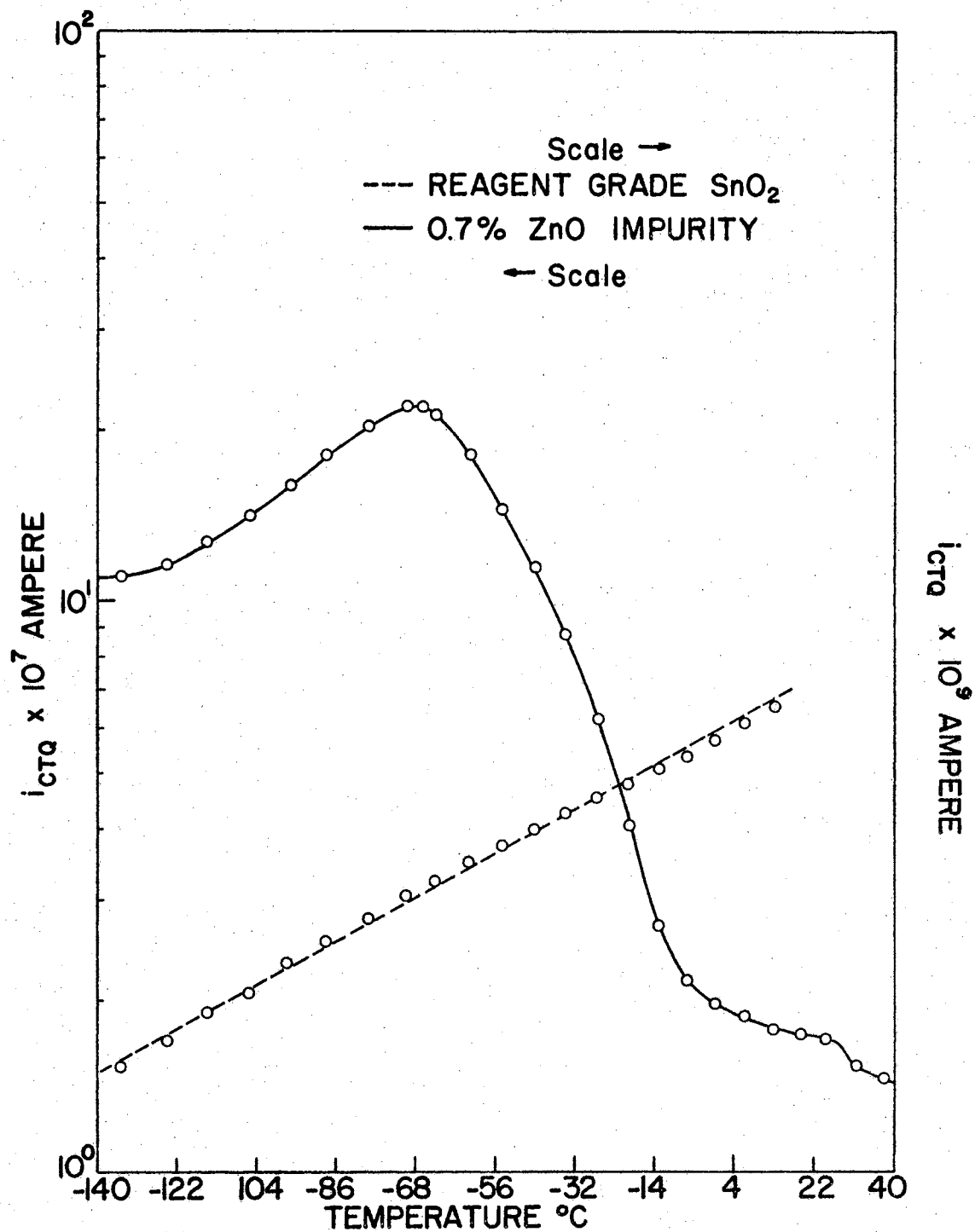


Figure 12. Continuous thermal quenching

## CHAPTER V

### CONCLUSIONS AND SUGGESTIONS FOR FURTHER STUDY

As emphasized in the introduction, a primary purpose of this investigation was to identify and study some experimental techniques which would appear particularly promising for providing basic material parameters through the interpretation of measurements done on ceramic (rather than single-crystal) specimens. Although many of the results were only qualitative in nature it is felt that they have established several avenues of future work which can be followed with profit. Specifically, this investigation will now be expanded to obtain quantitative photoelectronic analysis results and to examine certain interesting problems involved in ceramic fabrication. The following is a discussion of a few of these problems and of some of the experimental results described in the body of the report.

#### Firing and Forming Process

Although forming and firing of the ceramics seemed to be simply an experimental exercise in finding proper conditions for obtaining mature samples, these measurements suggested some fundamental questions about the basic nature of materials in ceramic form. Two of the most obvious are (a) How does the relative density of two samples affect a particular parameter such as the electrical conductivity or the dielectric constant? and (b) Why does the introduction of an impurity like

ZnO increase the densification and in what way is this increase dependent on the amount and kind of impurity? Presently samples containing a small amount of CuO impurity are being fabricated as the first step in a systematic study of both of these problems.

Another interesting phenomenon was the appearance of the pink color as mentioned in Chapter I. This color could possibly be associated with the presence of oxygen vacancies in the microcrystals although more work needs to be done to substantiate this contention. The color appears at  $\approx 1400^{\circ}$  C in the pure sample, and if there is to be no significant densification till  $1600^{\circ}$  C, then it seems that pure dense samples will only be obtained by sintering in an oxygen-rich atmosphere.

#### Microstructure of Ceramics

The microstructure of these ceramics needs further study. Although the measurements reported in Chapter III did show that a plausible explanation for the observed dispersion of dielectric constant and resistivity exists if one assumes a model of fused microcrystals, these measurements alone could not give any detailed picture of their intricate microstructure. In order to continue structural studies, it will be necessary to go to other methods such as electron microscope replica or optical micrograph techniques. Development of this area will further the systematic study of such basic problems in ceramics as the kinetics of grain growth and its importance to solid-state sintering.

#### Conductance Properties (Dark)

In discussing activation energies (see equation 6) obtained from dark current measurements, one must be careful to specify the thermal

history of the sample. Kunkle,\* working on artificial  $\text{SnO}_2$  crystals, has found large variations in calculated energy values depending on the thermal history and is attempting to correlate these variations with surface properties of the crystals. Since ceramics are essentially fused microcrystals, it follows that one must here too specify the pre-measurement conditions. Until this variation is better understood, values for  $E_a$  are quoted only for comparison purposes. In general these apparent activation energies decrease in magnitude through the sequence pure (white)  $\longrightarrow$  pure (pink)  $\longrightarrow$  zinc-doped specimens. It is not possible at this stage of the investigation to separate the effects of impurities, stoichiometry deviations, and bulk density differences which might account for these results.

#### Conductance Properties (Light)

The spectral response data reported in Chapter IV were taken at atmospheric pressure and room temperature. These measurements need to be expanded to see if there is any significant dependence on temperature of oxygen pressure.

As stated before, photodecay data do definitely show an oxygen pressure dependence. Preliminary analysis indicates a logarithmic decay process of a modified Elovich type and future studies will attempt to establish a firm relation between photoconductivity and chemisorption kinetics.

The thermally stimulated current data were the most dramatic and the most interesting. Here one could see peaks emerging two and three orders of magnitude from the dark conductivity, sometime rising and

---

\* H. Kunkle, unpublished results.

falling in less than  $15^{\circ}$  C. Two avenues for further study would seem particularly fruitful. Using the approach of Garlick and Gibson (15) based on the fact that thermally stimulated current rises exponentially on the low temperature approach to its peak, it would be possible to obtain more precise values for trapping energies by removing the necessity for taking geometrical factors into account and for assuming charge carrier mobility values. To eliminate the possible overlapping of peaks from several trapping levels though, it may be necessary to go to the decayed modification of this method as proposed by Bube (16). Once trapping level energies have been definitely identified, it will then be attempted to pinpoint their origins by systematically varying doping and surface treatment procedures and correlating these changes with thermally stimulated current results.

Although there were no numbers computed from the thermal quenching data, they showed vividly the sensitization of the samples due to the ZnO impurity. The next step will be to change the light intensity and get a family of curves from which one can calculate energies of the sensitizing centers. An effort will be made to find other dopants which have a large sensitizing effect and extend the sensitization temperature range.

## BIBLIOGRAPHY

1. Kohnke, E. E., J. Phys. Chem. Solids, 23 1557 (1962).
2. Kunkle, H. F., J. Appl. Phys., (to be published, 1965).
3. Loch, L. D., J. Electrochem. Soc., 1081 (1963).
4. Lewis, G. T., Unpublished Ph.D. dissertation, Alfred University (1964).
5. Hippel, A. V., Dielectrics and Waves, John Wiley and Sons, New York (1954).
6. Wyckoff, R. W. G., Crystal Structure, Interscience, New York (1951).
7. Peterson, A. L., Private communication.
8. Goodman, J. T. and Gregg, S. J., J. Chem. Soc., 1162 (1960).
9. Linder and Enquist, Arkiv För Kemi, 9, 471 (1956).
10. Nomura, S., J. Phys. Soc. Japan, 10 112 (1955).
11. Koops, C. G., Phys. Rev., 83 121 (1951).
12. Houston, J. E., "Photoelectronic analysis of imperfections in grown stannic oxide crystals," Technical Report No. 4, Contract No. Nonr-2595(01), Project NR 015 222, (1965).
13. Hurt, J. E., "Relation between photoconductivity and chemisorption kinetics for stannic oxide crystals," Technical Report No. 2, Contract No. Nonr-2595(01), Project NR 015 222, (1963).
14. Bube, R. H., Photoconductivity in Solids, John Wiley and Sons, New York (1960).
15. Garlick, G. F. J. and Gibson, A. F., Proc. Roy. Soc. (London) A60 574 (1948).
16. Bube, R. H., J. Appl. Phy., 35, 586 (1964).

VITA

Herman Excell Matthews, Jr.

Candidate for the degree of

Master of Science

Thesis: A PRELIMINARY STUDY OF CERTAIN ELECTRICAL PROPERTIES OF STANNIC  
OXIDE CERAMICS

Major Field: Physics

Biographical:

Personal Data: Born in Houston, Texas, March 16, 1940, the son of  
Herman and Cathrine E. Matthews.

Education: Graduate from Reagan High School in Houston, Texas, in  
1958; received a Bachelor of Science degree from Lamar Techno-  
logical College, with a major in Physics, in May, 1962.